Ocean Science Journal
https://doi.org/10.1007/s12601-022-00054-2

Online ISSN 2005-7172
Print ISSN 1738-5261

ARTICLE


# Estimation of Seagrass Biomass by In Situ Measurement and Remote Sensing Technology on Small Islands, Indonesia

Nurjannah Nurdin[1,2] · Khairul Amri[1] · Supriadi Mashoreng[1] · Teruhisa Komatsu[3,4]

Received: 8 June 2021 / Revised: 28 October 2021 / Accepted: 20 December 2021


**Abstract**
As one of the major blue carbon ecosystems, studying, conserving, and monitoring seagrass meadows, especially on small populated islands, has become very important due to their vulnerability to anthropogenic and global environmental factors. In this study, we used satellite image analysis and biological data to map seagrass percent cover (SPC), above-ground biomass (AGB), and below-ground biomass (BGB) on the three most populated islands of the Spermonde Archipelago, Indonesia, i.e., Kodingareng Lompo, Barrang Lompo, and Barrang Caddi. Reflectance and Normalized Difference Vegetation Index (NDVI) values of Sentinel-2 (S2) imagery were used to classify and calculate SPC and AGB. In situ biological data measurements were carried out from 3 to 14 of June, 2020, on the three islands to measure AGB and BGB. The result from image classification shows a total area of 126.37 Ha of seagrass, which was divided into three SPC categories: medium (30–59.9%) with a total area of 78.38 Ha; low (0–29.9%) with a total area of 13.1 Ha; and high (60–100%) with a total area of 34.89 Ha. The highest SPC area was observed on Kodingareng Lompo Island with 61.07Ha, followed by Barrang Lompo Island with 53.18Ha, and Barrangcaddi Island with 12.12Ha. The total AGB on Barrang Lompo, Kodingareng Lompo, and Barrangcaddi in tons of dry weight/ha were 1.83, 1.05, and 2.38, respectively. The highest BGB was reported on Barrangcaddi Island with 8.61 tons of dry weight/ha, followed by Barrang Lompo Island with 6.78 tons of dry weight/ha, and Kodingareng Lompo Island with 2.78 tons of dry weight/ha. Regression analysis showed a linear correlation between NDVI value and in situ SPC with $R^2 = 0.8255$. The framework of this study can be applied to monitor temporal changes of seagrass meadows distribution on small islands to promote a more sustainable ecosystem.

**Keywords** Biomass · NDVI · Seagrass · Sentinel-2 · Small islands

## 1 Introduction

Seagrass meadows have a high carbon sink capacity that surpasses even highly productive terrestrial ecosystems (Krause-Jensen and Duarte 2016). Seagrass meadows have a carbon fixation ability that exceeds their metabolic needs; hence, a large proportion of excess organic carbon is transported to the roots and rhizomes where it is stored and eventually exuded in the sediment to form anaerobic organic-rich soil (autochthonous) (Lyimo 2016). A study of the carbon sequestered capacity of Australian seagrasses estimates annual organic carbon ($C_{org}$) accumulation to be between 0.093 and 6.15 Mt, with a most probable estimation of 0.93 Mt year$^{1}$ (10.1 t km$^{-2}$ year$^{-1}$) (Lavery et al. 2013). This type of blue carbon ecosystem also has a high global net carbon production (NCP) of 20.73–50.69 Tg C year$^{-1}$, which comprises 10–18% of the total carbon storage in the ocean (Duarte et al. 2010; Kennedy et al. 2010).

However, disturbances caused by humans can negatively influence the carbon fixation ability of seagrasses and affect the amount of carbohydrate and starch being stored in their rhizomes. Growing in coastal environments, seagrasses are

✉ Nurjannah Nurdin
nurj_din@yahoo.com

[1] Faculty of Marine Science and Fisheries, Hasanuddin University, Makassar 90245, Indonesia

[2] Research and Development Center for Marine, Coast and Small Islands, Hasanuddin University, Makassar 90245, Indonesia

[3] Atmosphere and Ocean Research Institute, The University of Tokyo, Kashiwa 277-8564, Japan

[4] Present Address: Japan Fisheries Resource Conservation Association, Tokyo 104-0044, Japan

Published online: 04 February 2022

usually subjected to many anthropogenic activities e.g., sewage disposal, mariculture, propeller boating activities, destructive fishing, construction works, dredging, and eutrophication, which threatens their ecosystems and can lead to extinction (Roca et al. 2016). It is believed that about a third to half of the world's seagrasses have been lost since 1879 and the continuing rate of disappearance is estimated to be 110 $km^2$ per year with net loss rates of 0.9% per year before 1940 to 7% since 1990 (Waycott et al. 2009). Therefore, the remaining seagrass ecosystems need to be conserved and protected.

Information on seagrass status in terms of percent cover and biomass needs to be acquired as baseline data to efficiently manage and monitor the seagrass ecosystems for conservation purposes. Remote sensing techniques have proven to be efficient and effective tools for seagrass monitoring. Since launched by the European Space Agency (ESA) in 2015, Sentinel-2 (S2) images with higher spatial resolution that are suitable for seagrass mapping, have been available and can be acquired at no cost. The use of S2 imagery for seagrass meadows ecosystem study was recently demonstrated with regard to seagrass beds on the Atlantic coasts of France and Spain (Zoffoli et al. 2020).

Spermonde Archipelago is a set of small tropical islands between Kalimantan and Sulawesi islands in Indonesia. Three of its most populated islands are Barrang Lompo, Barrang Caddi, and Kodingareng Lompo. Despite high anthropogenic disturbance factors most likely occurring on these islands, there are still significant amounts of seagrass ecosystems that can be found on these islands. However, a study to analyze the percent cover and biomass of these seagrasses has not been done yet. The main objective of this study is to map seagrass distribution and the total areas on the three most populated islands in the Spermonde Archipelago using two different spatial resolution imageries, Sentinel-2 and Landsat 8. Several variables, including seagrass density and biomass, were measured directly in the field to find a correlation between in situ values and NDVI values derived from Landsat 8 and Sentinel-2 image analysis.

## 2 Materials and Methods

### 2.1 Study Sites

This study was conducted on three islands: Barrang Lompo (BL), Barrang Caddi (BC), and Kodingareng Lompo (KL). These three islands are part of the Spermonde Archipelago, which is located west off the coast of Makassar City, capital of South Sulawesi Province, Indonesia. BL Island is located at 5° 2′ 43.577″–5° 3′ 6.491″ South latitude (SL) and 119° 19′ 38.716″–119° 19′ 49.21″ East longitude (EL), which is 12.48 km from Makassar City. Meanwhile, BC Island is located at 5° 4′ 46.558″–5° 5′ 0.778″ SL and 119° 19′ 10.557″–119° 19′ 16.21″ EL with a distance of 10.98 km from Makassar City, while Kodingareng Lompo Island is located at 5° 8′ 42.536″–5° 9′ 9.434″ SL and 119° 15′ 45.006″–119° 15′ 58.540″ EL with a distance of 15.24 km from Makassar City. Based on the distance from the mainland, the three islands were included in the middle zone, with the distance from the mainland coastline between 10 and 20 km (Fig. 1). Field data were taken at BL, BC, and KL islands from 3 to 14 June 2020. Data derived from satellite images used for this study were acquired from S2 on July 29th 2019 and from Landsat 8 (L8) on January 6th 2019.

### 2.2 Satellite Data

#### 2.2.1 Landsat 8 and Sentinel-2 Image Pre-processing

Satellite image data used in this study were acquired from S2 on July 29th 2019 and L8 on January 6th 2019. Geometrically corrected S2 images of waters west of South Sulawesi were downloaded from the European Space Agency (ESA) data portal, while images from Landsat 8 were downloaded from USGS Glovis. Atmospheric correction was conducted using radiometric calibration (DN to reflectance) and DARK OBJECT SUBTRAction (DOS) to remove the atmospheric effect on the images, assuming the darkest pixel value was zero (Chavez. 1988). Sun glint correction was applied on S2 imagery to correct sunlight reflection. This correction was not performed on L8 imagery as the images were clear enough; however, a pan-sharpening technique was performed to facilitate interpretation for image classification. Sun glint correction for S2 imagery was carried out using an algorithm developed by Hochberg and Atkinson(2003) and refined by Hedley et al. (2005) as in the following equation:

$$R'_i = R_i - b_i(\mathrm{RNIR} - \mathrm{MinNIR}), \quad (1)$$

$R'_i$ is the $i$ channel value after being reduced; $R_i$ is the initial $i$ channel value; $b_i$ is the amount of slope of the regression; RNIR is the NIR channel value; MinNIR is the minimum NIR channel value.

Athmospheric corrections and water column correction were applied to the images to classify shallow-water habitats and seagrass percent cover (SPC) using supervised classification. The flowchart for spatial data processing and its integration with non-spatial data can be seen in Fig. 2.Water column correction method was applied to the images using depth invariant index (DII) algorithm by Lyzenga (1981). The DII method reduces the influence of the water column so that clearer images of shallow water habitats could be obtained. Points on the sand area were used to build a model to obtain the attenuation coefficient of the water column. This is because sand objects are easier to recognize in the images, with the bright white appearance

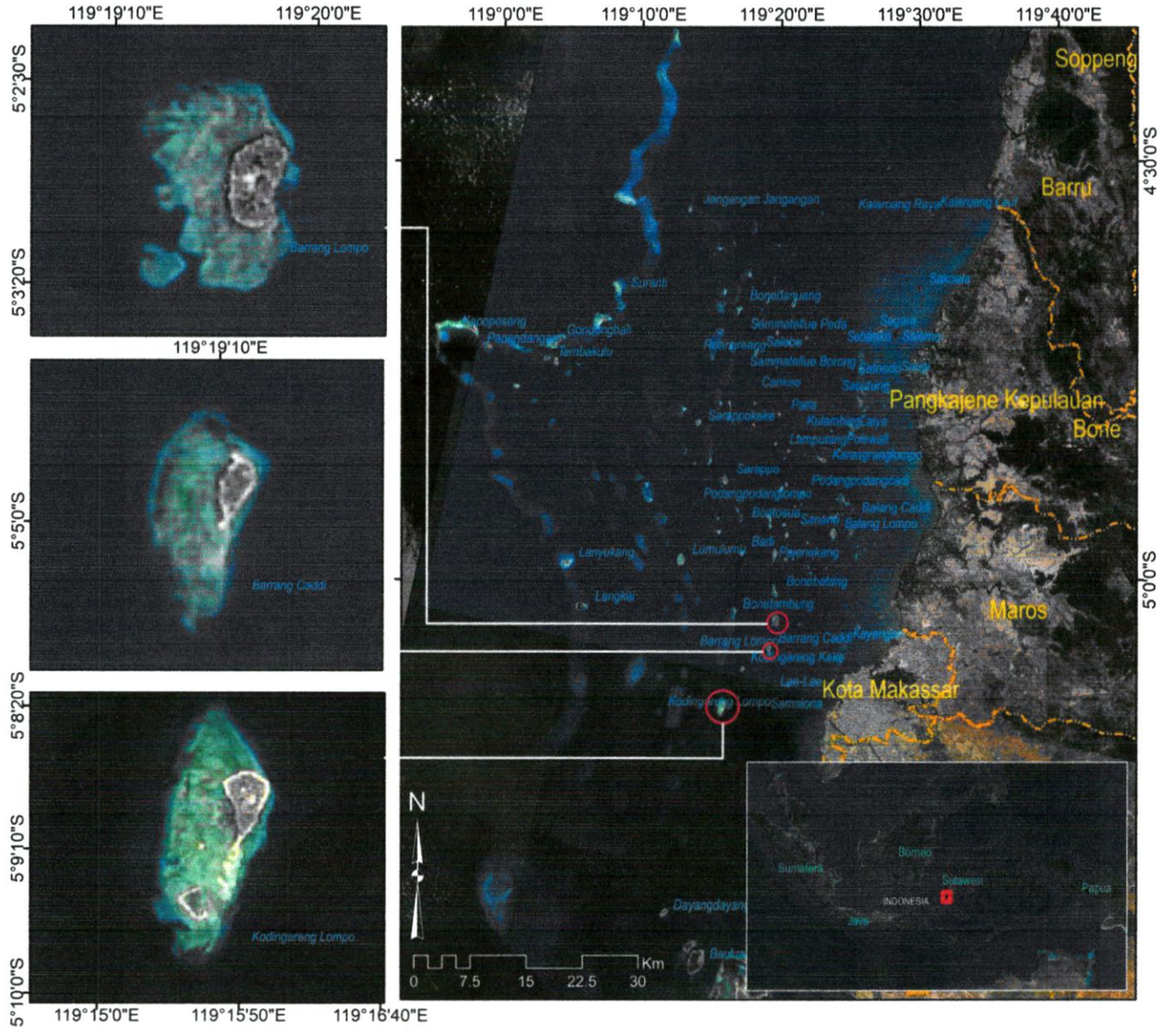


**Fig. 1** Study site on BL (Barrang Lompo), BC (Barrang Caddi), and KL (Kodingareng Lompo) islands, Spermonde Archipelago, South Sulawesi, Indonesia

becoming a darker blue color as the water depth increases. The algorithm used in this process was:

$$\mathrm{DII}(ij) = \ln\left(L_i\right) - \left[\left(K_i/K_j\right)\ln\left(L_j\right)\right], \tag{2}$$

$$k_i/k_j = a - \left[\left(K_i/K_j\right)\ln\left(L_j\right)\right], \tag{3}$$

$$\alpha = \frac{\sigma_i+\sigma_j}{2\sigma_{ij}}. \tag{4}$$

DII is the depth invariant index; $L_i$ is the $i$-band reflectance value; $L_j$ is the $j$-band reflectance value; $k_i/k_j$ is the $i$ and $j$ band attenuation coefficient ratio; $\alpha_i$ is the $i$-band variant; $\alpha_j$ is the $j$-band varian; $\alpha_{ij}$ is the $i$ and $j$ band covariant.

### 2.2.2 Image Classification Based on SPC

Images that have been corrected were then classified using an unsupervised classification method (Isoclass). The results were then reclassified based on ground truth data. The final classification of SPC was divided into three categories i.e., low (0–29.9%), medium (30–59.9%), and high (60–100%). These categories were then used to determine biomass sampling points.

The classification mapping accuracy was tested using a confusion matrix method to calculate the accuracy value of

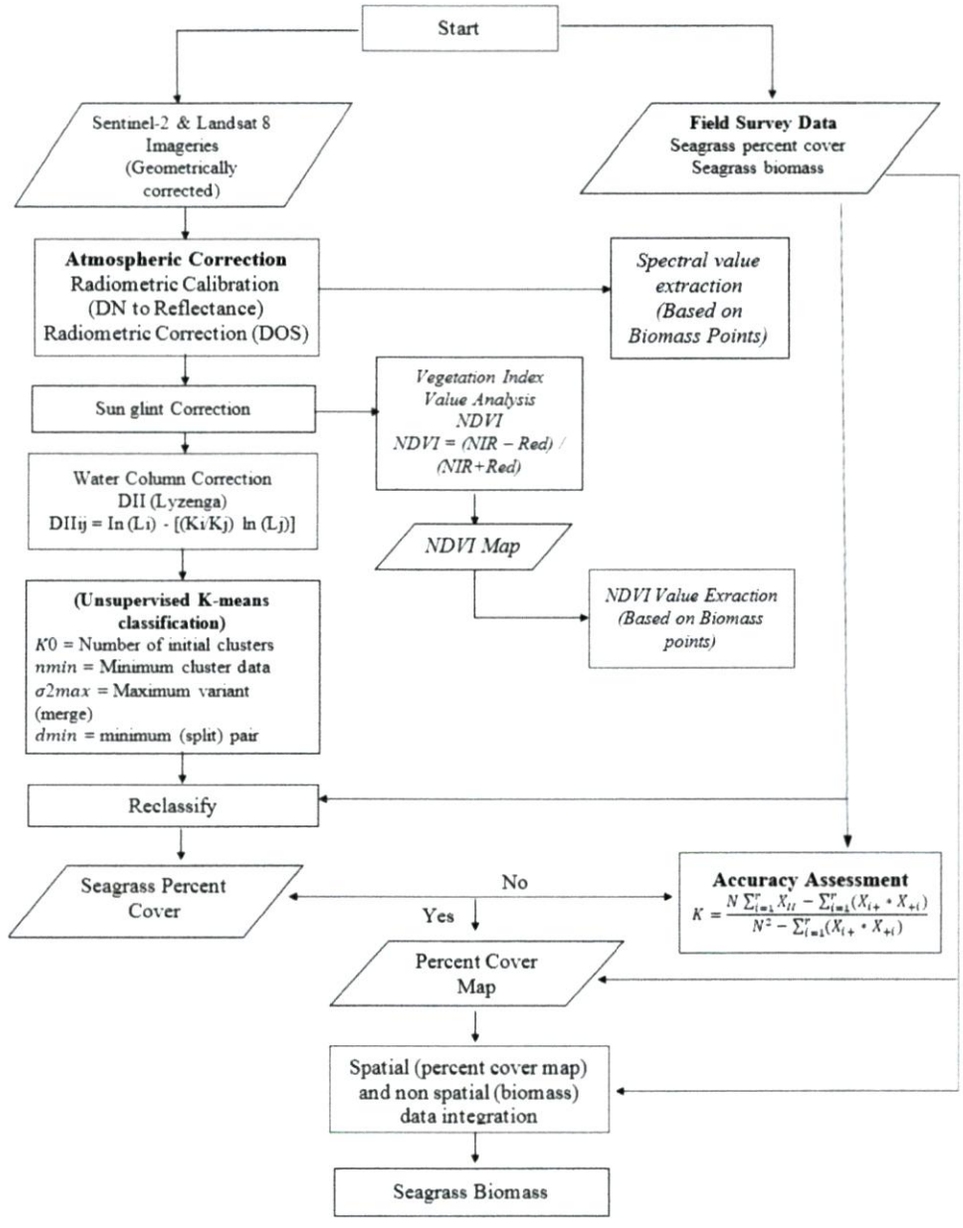


**Fig. 2** Flowchart analysis of integration image and in situ data to seagrass biomass

seagrass habitat mapping. It was done using a matrix table that compares classes from satellite image classification with in situ data (Congalton and Green 2008). The error matrix method used in this study followed the following formula:

$$K = \frac{N\sum_{i=1}^{r} X_{II} - \sum_{i=1}^{r}\left(X_{i+} \times X_{+i}\right)}{N^2 - \sum_{i=1}^{r}(X_{i+} \times X_{+i})}. \quad (5)$$

### 2.2.3 Image Classification Based on Seagrass Density

The NDVI (normalized difference vegetation index) algorithm has been used to measure vegetation density level (greenness) using the reflectance values of the near-infrared (NIR) and red bands (Pu et al. 2015). Seagrass beds usually grow in shallow waters, with the NDVI index value ranging from − 1 to 0. The formula used for NDVI was:

$$\mathrm{NDVI} = \frac{\mathrm{NIR} - \mathrm{Red}}{\mathrm{NIR} + \mathrm{Red}}. \quad (6)$$

NDVI is the normalized difference vegetation index; NIR is the short infrared band spectral reflectance; Red is the red band spectral reflectance.

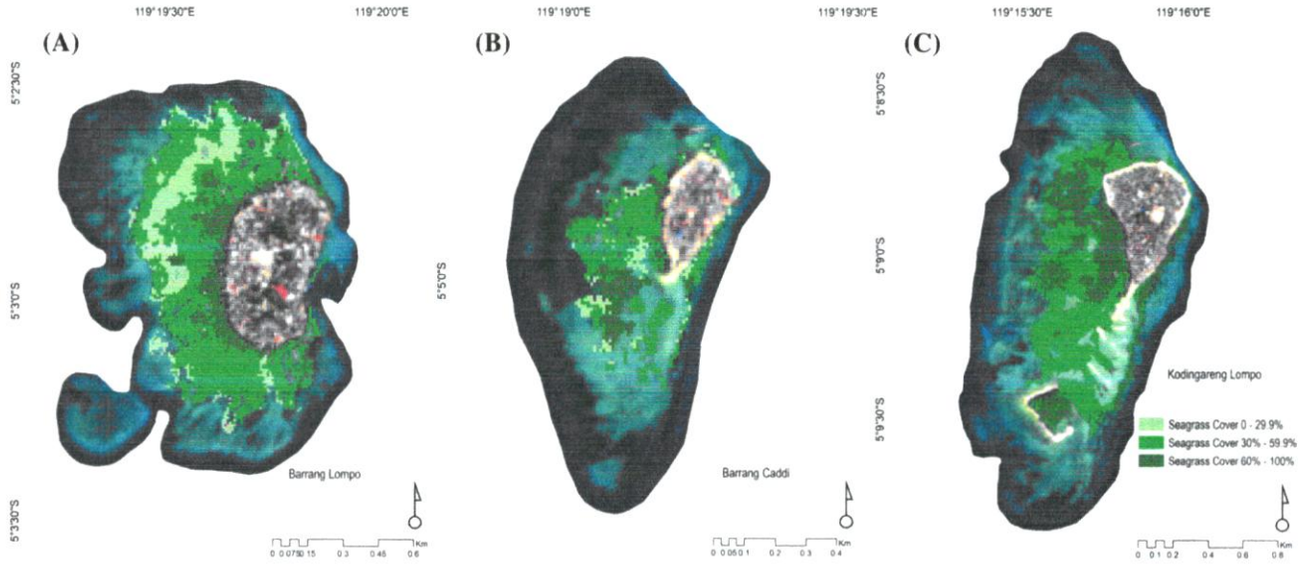


**Fig. 3** Seagrass distribution maps of **A** Barrang Lompo, **B** Barrang Caddi, and **C** Kodingareng Lompo using 10 m spatial resolution Sentinel-2 imagery, with the acquisition date on July 29th 2019. Seagrass were categorized into three classes, i.e., 0–29.9% (low), 30–59.9% (medium) and 60–100% (high)

## 2.3 Field Data

### 2.3.1 In Situ SPC and Biomass Sampling

Based on the unsupervised SPC image classification, 60 stations were designated on each island as the sampling points (20 for each SPC categories i.e., low, medium, and high). In situ measurements of SPC and seagrass density were carried out using a 50 cm × 50 cm plot (McKenzie et al. 2001). Seagrass species were also identified in every plot. A smaller plot (20 cm × 20 cm plot) was placed within the bigger plot to measure seagrass biomass. The plot was placed based on the types of seagrasses that exist within the bigger plot so that all types of seagrasses in the plot could be extracted. Seagrass biomass samples were collected with roots up to 40 cm long. Vined rhizomes were chopped using a machete before picking out any sample. Seagrass samples consisting of roots, rhizomes, leaves, and midribs were collected from each station. Substrate and dirt were cleaned away from the samples and then each of them was put into a labeled plastic bag for further laboratory analysis.

### 2.3.2 Biomass Analysis

In the laboratory, samples were cut into two parts, the biomass above the sediment or above ground biomass (AGB) which consists of leaves and leaf midribs, and the below-ground biomass (BGB) which consists of rhizomes and roots (Rohr et al. 2018). The samples were then oven-dried (60 °C) until a constant weight was achieved (Lyimo 2016). Samples were then weighted using a 0.01-g precision level digital scale. Seagrass biomass per shoot was calculated by dividing the total weight of each sample by the total number of its shoots. The mean biomass per area ($g/m^2$) for each seagrass percent cover category was obtained by multiplying the number of biomass per shoots with each type of seagrass density. The result value was then multiplied by the area of each of the percent cover categories to get the total biomass per category.

### 2.3.3 Regression Analysis

The corelation between biomass (AGB, BGB, and total biomass) and the SPC results on every island was determined using regression linear analysis. Regression analysis was also performed to find the corelation between field survey data (in situ percent cover and biomass) with spatial data (percent cover and NDVI value).

# 3 Result and Discussion

## 3.1 SPC Based on Image Classification

The seagrass maps were generated using a pixel-based classification method (unsupervised classification). 3 highly populated islands in the Spermonde Archipelago were analyzed in this study. Based on the results, SPC in KL was mainly in the range between 30 and 59.9% (medium), which accounts for 60.38% of the total seagrass area on this island. Similarly, SPC on BC and BL islands were also mainly characterized by the medium SPC category, which accounts for 62.71% and 63.74%, respectively, of the total seagrass areas that were

**Table 1** Percent cover of seagrass area from Sentinel-2 imagery classification

| Seagrass percent cover (%) | Area (ha) |
|---|---|
| 0–29.9 (low) | 13.1 |
| 30–59.9 (medium) | 78.38 |
| 60–100 (high) | 34.89 |
| Grand total | 126.37 |

**Table 2** Total seagrass area by Landsat 8 and Sentinel-2

| Island | Area by Landsat | | Area by Sentinel-2 | |
|---|---|---|---|---|
| | Area (ha) | Years | Area (ha) | Years |
| BL | 37.66 | 2019 | 53.18 | 2019 |
| BC | 9.61 | 2019 | 12.12 | 2019 |
| KL | 46.30 | 2019 | 61.07 | 2019 |

identified on each island. Overall, medium SPC category accounts for 62.02% of the total seagrass area identified on these three islands (Fig. 3; Table 1). Spermonde Archipelago has 683.70 ha of seagrass, so it can be said that these three islands contribute around 18.48% of the total seagrass in the Spermonde Archipelago.

Pixel-based analysis was also applied on L8 images to create seagrass distribution maps on each island (Fig. 4). Due to its lower spatial resolution (30 m), seagrass mapping using L8 was only up to the aquatic habitat condition or seagrass distribution that was able to be classified using L8 (Fig. 4; Table 2). Nevertheless, the results between L8 and S2 show similar seagrass spatial distribution. As can be seen in Figs. 3 and 4, seagrass is dominantly grown in the western area of the islands, while the eastern part remained barren.

There were differences in total seagrass areas calculated with L8 and S2 image processing. Calculation with S2 resulted in a larger seagrass area by 24.2% on KL Island, 20.7% on BC Island, and 60.9% on BL Island compared with L8. Seagrass maps of KL and BC islands show that each island has several dominant and sparse seagrass distribution spots (Table 1). The seagrass-dominant areas at KL and BC islands were mostly on the west, southwest, to the south of the island, while on the north to the east side of the islands, the seagrass distribution was mostly sparse. Identification from the survey and aerial images indicate that lack of seagrasses on the east sides of the islands was due to water depth and human activities mostly centered on the east side of the island (the side that faces the mainland). This side was the main channel for local passenger ships (Fig. 5: A1, B1, C1) and the port area of each island.

The south side of BC and KL islands were mostly covered with white sands which were exposed during low tide and, therefore, not suitable for seagrass to grow. Seagrass distribution on BL Island was almost evenly distributed on each side of the island, except at the areas around the main port. BL is a highly populated island and packed with house settlements. People often dispose their household organic waste on the west side of the island, with the waste entering straight into the sea and the same thing occurs on the other islands. Hence, due to this activity, disposed organic materials on this side of the island has resulted in increasing organic nutrients inputs which support seagrass growth. As can be seen in the Fig. 5A2, 5B2, and 5C2 there are

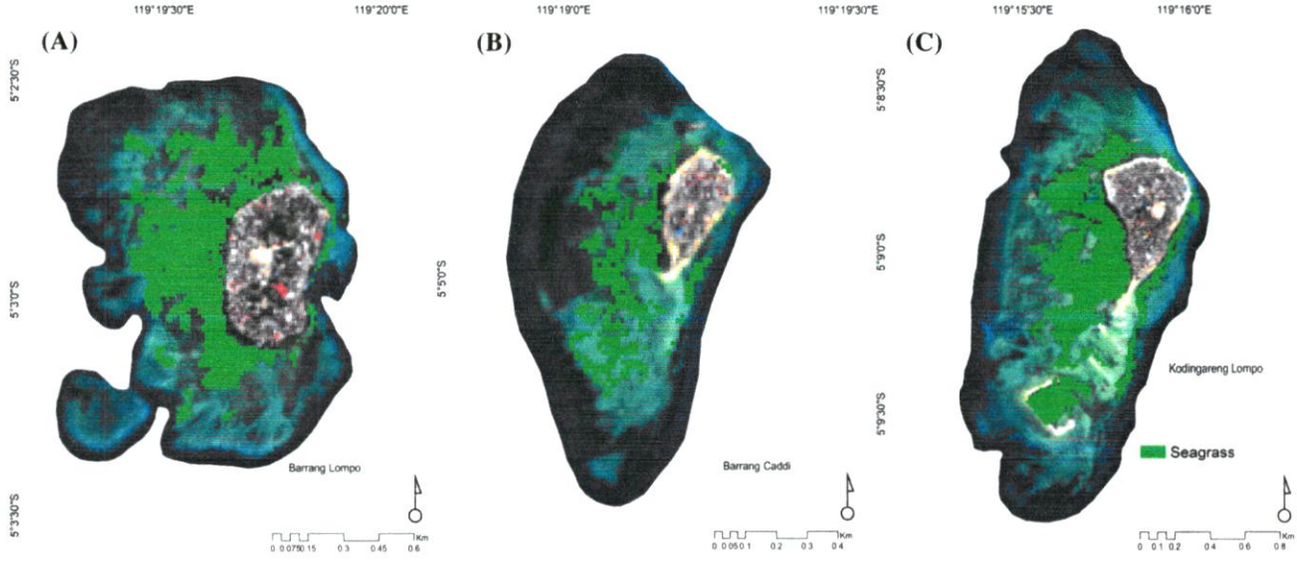


**Fig. 4** Seagrass distribution maps of **A** Barrang Lompo, **B** Barrang Caddi, and **C** Kodingareng Lompo using 30 $m^2$ spatial resolution Landsat 8 OLI Imagery acquired on January 6th 2019

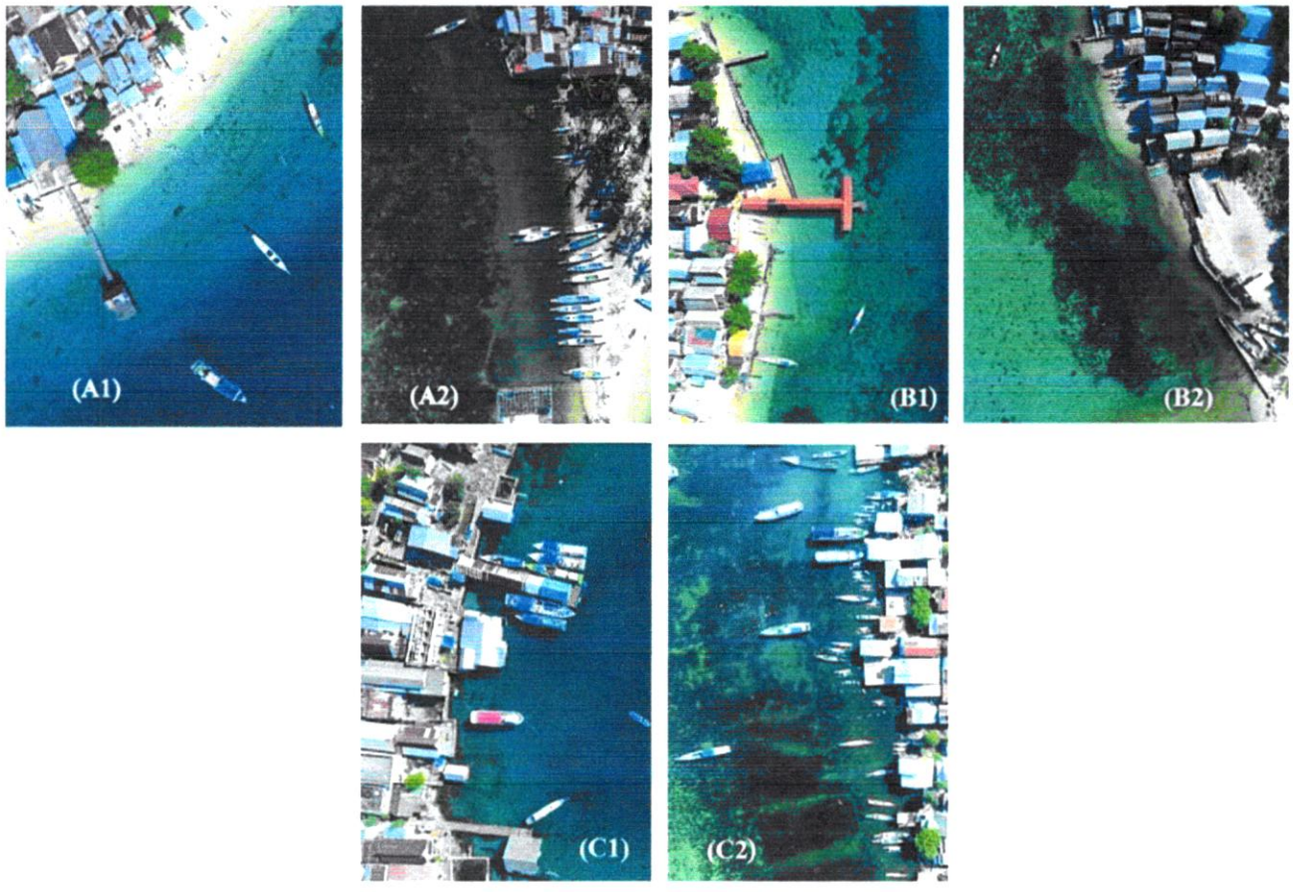


**Fig. 5** Aerial photographs showing the shallow water condition on the east and the west side of Kodingareng Kompo (**A1–A2**), Barrang Caddi (**B1–B2**) and Barrang Lompo (**C1–C2**) islands. The east sides of the islands (**A1**, **B1** and **C1**) showed less seagrass beds than the west sides of the islands (**A2**, **B2**, **C2**)

more seagrass beds that can be observed on the west sides of these islands due to the disposal of richer organic materials compared to the east sides (Fig. 5A1, 5B1, 5C1). Nutrient enrichment enhanced seagrass biomass density, particularly in increasing the shoot biomass (Cabaco et al. 2013).

### 3.2 Accuracy Test

The accuracy test of the S2 image classification results was obtained using field data. Field data used was a sample of seagrass cover photos that have coordinates. Based on the image analysis results, the overall accuracy of the kappa value of each image was: KL Island 75%, BC Island 82.69%, and BL Island 80.60%.

### 3.3 Seagrass Percent Cover (SPC) and Density from In Situ Measurement

The result from in situ measurement shows that seagrass density and SPC have a synched pattern, from low to high density, and low, medium, and high categories, respectively (Table 3). In some cases, the seagrass density value may be higher in the percent cover high category than in the medium or low category. The consistent pattern of seagrass density in all three islands is more likely due to the relatively similar composition of seagrass species in the three percent cover categories.

Six species of seagrass were found on the three islands, i.e., *Enhalus acoroides*, *Thalassia hemprichii*, *Cymodocea rotundata*, *Halodule uninervis*, *Halophila ovalis* dan *Syringodium isoetifolium*. Seagrass composition was dominated by *T. hemprichii* in all categories. An exception was found on KL Island where *C. rotundata* dominated the low category (Fig. 6).

### 3.4 Correlation Between Density of Seagrass Using NDVI Algorithm and Percent Cover of Seagrass Using In situ Data

NDVI has been widely used in several studies in Indonesia to estimate vegetation biomass, greenness level, primary production, and dominant species in vegetation. The NDVI index value

**Table 3** Seagrass density and percent cover from in situ measurement

| Plot Category | Density (shoots/m$^2$) | | | Percent cover (%) | | |
|---|---|---|---|---|---|---|
| | BL | BC | KL | BL | BC | KL |
| High | 418.2 | 447 | 310.733 | 78.25 | 76.9 | 77.867 |
| Medium | 367.6 | 411.8 | 229.6 | 45.45 | 38.95 | 46.267 |
| Low | 239.6 | 178.2 | 268.235 | 23.9 | 18.6 | 20 |

*BL* Barrrang Lompo, *BC* Barrang Caddi, *KL* Kodingareng Lompo

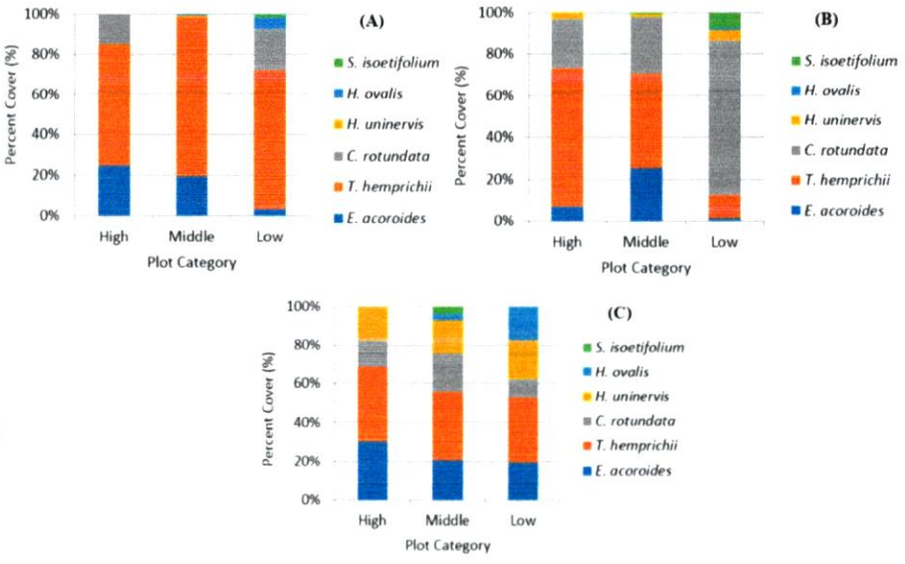


**Fig. 6** Percent cover of each seagrass 'species' based on plot categories in **A** Barrang Lompo, **B** Kodingareng Lompo, and **C** Barrang Caddi

ranges from -1.00 to 1.00. The principle of NDVI is to measure the level of greenness intensity. The intensity of greenness in Sentinel-2 (Fig. 7) and Landsat 8 (Fig. 8) images correlates with the level of density of the vegetation canopy.

The relationship between SPC from field measurements and NDVI values was analyzed using algorithmic modeling with linear regression. The regression equation was obtained from the relationship between the NDVI value of S2 images and the value of in situ SPC. The algorithm obtained was $y=0.0053x-0.785$. Regression analysis shows a linear correlation between NDVI and in situ data with $R^2$ value of 0.8255. The $R$ value indicates a strong relationship between the in situ SPC and the NDVI values of satellite images (Fig. 9).

## 3.5 Seagrass Biomass

### 3.5.1 Total Biomass

Results from laboratory analysis showed seagrass BGB in all islands and in each seagrass cover category were higher than AGB. Seagrass BGB value on BL island on average was four times higher than AGB. Meanwhile, the ratio was smaller on the other two islands, which was about three to three and a half times higher (Table 3). Biomass stored under the substrate is one of the forms of seagrass adaptation. Seagrass grows in shallow waters, which makes it very vulnerable to the influence of waves. Without specific adaptation, seagrass can be easily uprooted by the waves. Seagrass adapts by storing more photosynthetic products under the ground than above, therefore, it can stay still under the impact of waves.

Among the three islands, the highest average biomass was found on BC Island, either for BGB, AGB, or the total biomass (Table 4). This is more likely due to the large composition of *E. acoroides*, especially in the high-percent cover category. The percent cover of *E. acoroides* reached 23.2% or about 30% of the total seagrass cover in the high category of the island. *E. acoroides* is a large seagrass species (Waycott et al. 2004) and the largest seagrass species that can be found in Indonesia.

Seagrass BGB was generally weighted higher than ABG in the seagrass categories on the three islands. High categories dominated seagrasses on the three different islands. There was a total of 8.62 ton dry weight/ha seagrass biomass on BL Island, 3.83 ton dry weight/ha on KL Island, and 10.99 ton dry weight/ha on BC Island (Fig. 10).

### 3.5.2 Correlation Between Biomass In Situ and NDVI

The correlation between the total biomass and the NDVI values of the three islands was analyzed. $R^2$ values acquired from regression analysis were 0.40 for Landsat 8, and 0.43

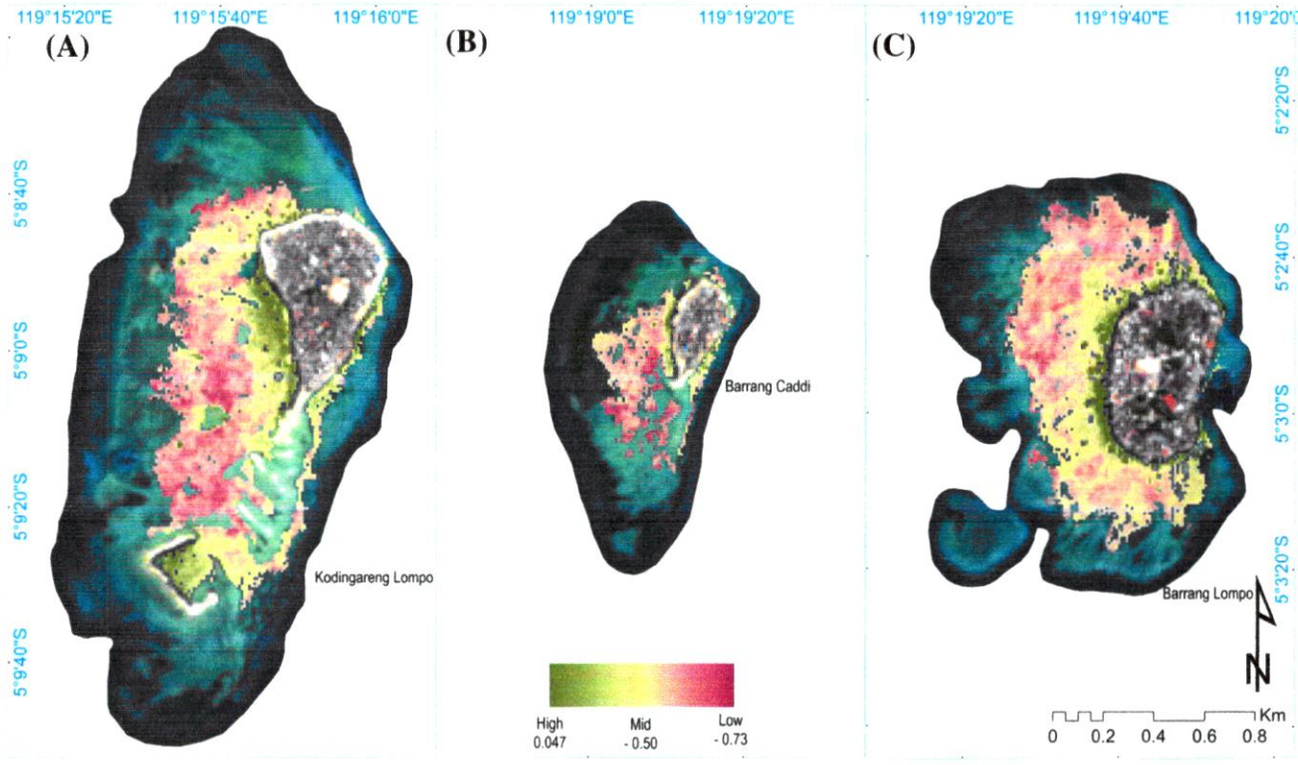


**Fig. 7** NDVI values derived from Sentinel-2 on Kodingareng Lompo (**A**), Barrang Caddi (B) and Barrang Lompo (**C**)

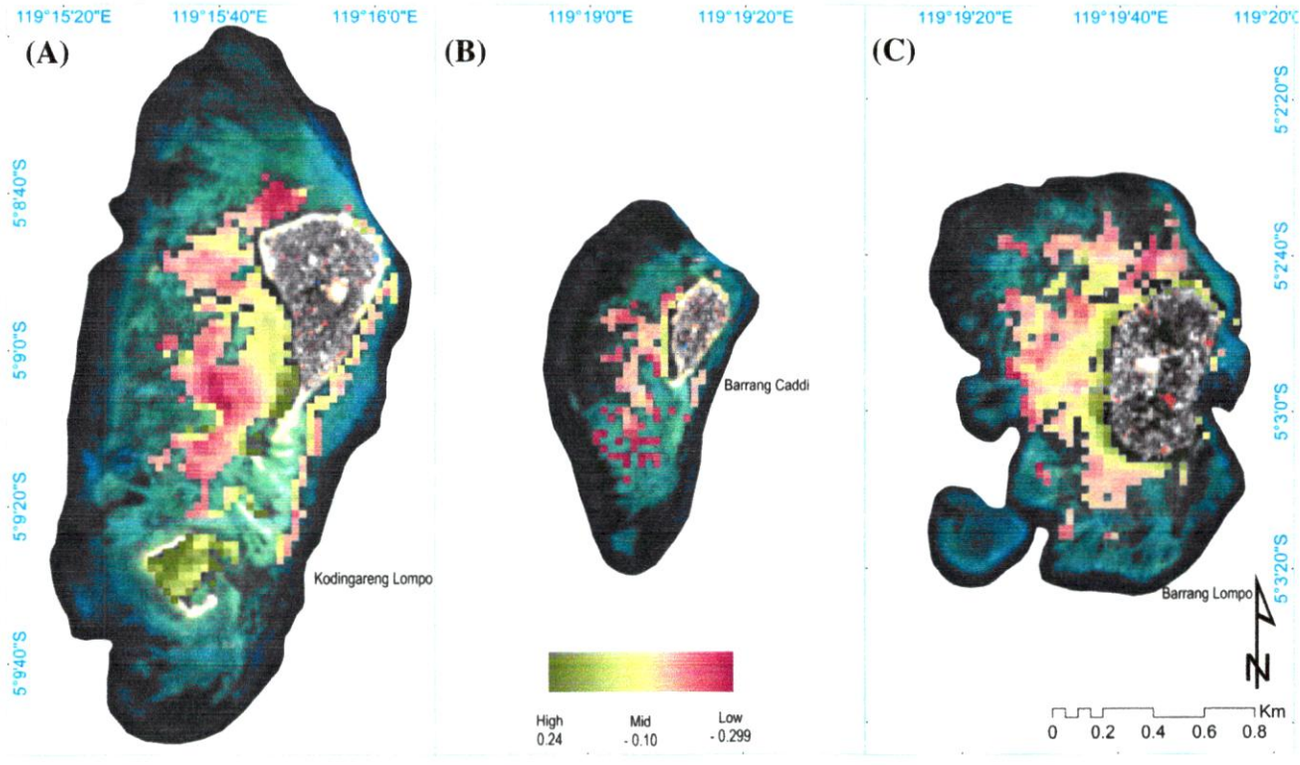


**Fig. 8** NDVI derived from Landsat 8 on Kodingareng Lompo (**A**), Barrang Caddi (**B**) and Barrang Lompo (**C**)

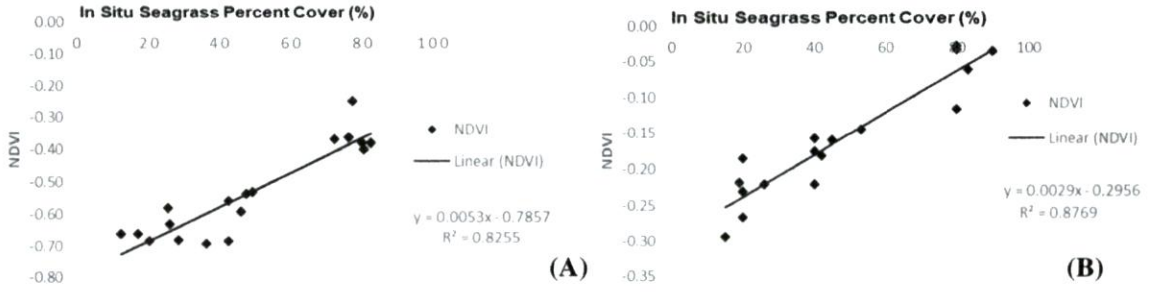


**Fig. 9** Correlation analysis of SPC between in situ measurement and NDVI values on the three islands; **A** Sentinel-2 imagery, **B** Landsat 8 imagery

**Table 4** Seagrass biomass in the study locations based on high, medium, and low categories

| Location | Category | Biomass (dry weight ton /ha) | | |
|---|---|---|---|---|
| | | Above ground | Below ground | Total |
| Barrang Lompo | High | 1.05 | 3.49 | 4.55 |
| | Medium | 0.58 | 2.33 | 2.9 |
| | Low | 0.2 | 0.96 | 1.17 |
| Kodingareng Lompo | High | 0.48 | 1.28 | 1.76 |
| | Medium | 0.46 | 1.01 | 1.47 |
| | Low | 0.11 | 0.49 | 0.6 |
| Barrang Caddi | High | 1.33 | 4.83 | 6.16 |
| | Medium | 0.75 | 2.75 | 3.5 |
| | Low | 0.3 | 1.03 | 1.33 |

for Sentinel-2. These $R^2$-values indicate a low correlation between the total biomass value and the NDVI value. Overall, NDVI and carbon biomass of seagrass showed a linear relation (Fig. 11). The higher the total biomass value, the closer the NDVI value will be to 0 (solid seagrass cover condition), while the lower the total biomass value, the closer the NDVI value will be to − 1 (low seagrass cover condition).

Moreover, on BL Island, the biomass value has more variation in the high seagrass cover category than in the low and medium categories (Table 4). This is due to the various species composition. Some plots were *T. hemprichii* dominant, while other plots were more *E acoroides* dominant. Morphologically, the two seagrasses have different sizes, therefore, at the same cover percentage, they have very different biomass values. In the low and medium seagrass cover categories, *T. hemprichii* was consistently the dominant species.

Furthermore, in the high seagrass cover category, there was quite a lot of overlap between leaves, especially with the *T. hemprichii* species. In some plots (Fig. 10), a large addition of seagrass cover value can only cause a small increase in biomass value. Meanwhile, in other plots, the addition of the same amount of seagrass cover value can add a substantial biomass value. However, in the high and medium seagrass cover categories, the overlap between leaves was less. According to Mallombassi, et al (2020), the high slope value of *T. hemprichii* seagrass regression equation at high percent cover was because of the overlapping leaf canopy, resulting in a high increase of biomass value despite the small addition of the percent cover.

*E. acoroides* and *C. rotundata* significantly contributed to the medium to sparse percent cover category on KL and BC islands. This causes the biomass values of those two

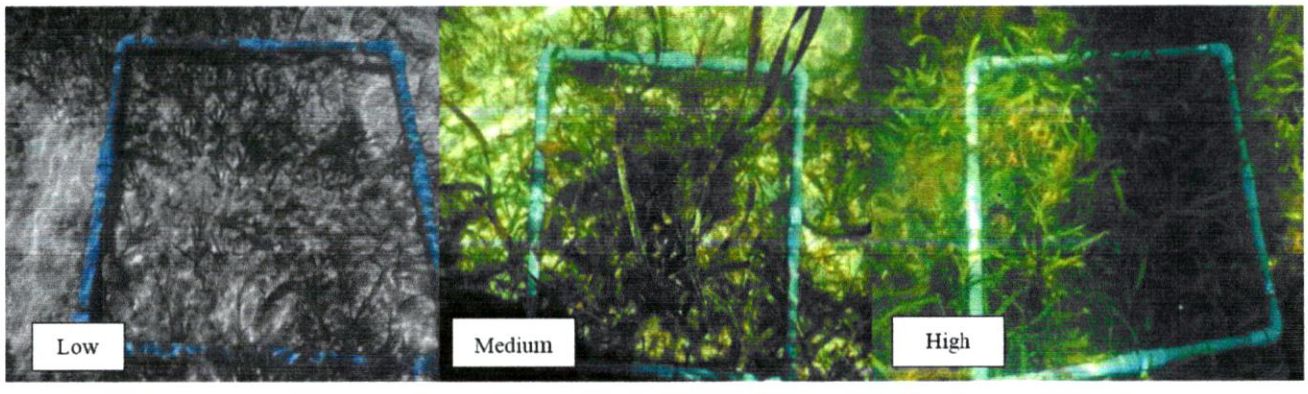


**Fig. 10** Field photographs of the low, medium, and high seagrass categories on Kodingareng Lompo and Barrang Lompo

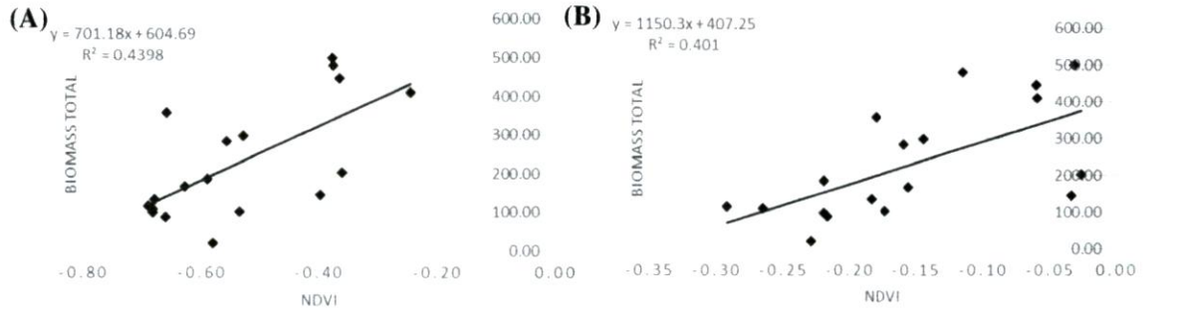


**Fig. 11** Regression analysis of seagrass biomass and NDVI on Barrang Lompo, Barrang Caddi, and Kodingareng Lompo islands; **A** Sentinel-2 imagery, **B** Landsat 8 imagery

categories to vary largely. The contribution of the two seagrasses was about half of the dominant species *T. hemprichii*, while on BL Island, it can reach a quarter in the same category.

## 4 Conclusions

The result of this study showed that there is a strong correlation between in situ seagrass percent cover and NDVI values derived from the two satellite images. However, the correlation between in situ seagrass total biomass and the NDVI values showed a relatively weak correlation. Image classification showed that seagrass was distributed mostly on the west side of the islands, and there were six seagrass species identified on the sites, i.e., *E. acoroides*, *T. hemprichii*, *C. rotundata*, *H. uninervis*, *H. ovalis* and *S. isoetifolium*. In this study, we also discovered that there was a disparity of seagrass total cover area between Sentinel-2 and Landsat 8, due to spatial resolution diferrences. Sentinel-2 images were able to classify seagrass distribution up to the seagrass density category, however, they cannot be applied to differentiate seagrass density based on species. Nevertheless, both Sentinel-2 and Landsat 8 are useful for seagrass condition monitoring purposes.

**Acknowledgements** The Ministry of Research Technology and Higher Education of the Republic of Indonesia and Institute for Research and Community Services, Hasanuddin University grant 2021–2022 for their support in providing research funds. Thank you to the Ocean Remote Sensing Project of the Sub-commission of the Western Pacific Intergovernmental Oceanographic Commission/ UNESCO supported by Japan Fund in Trust provided by the Ministry of Education, Culture, Sports, Science and Technology, Japan.

## References

Cabaço S, Apostolaki ET, García-Marín P, Gruber R, Hernández I, Martínez-Crego B, Mascaró O, Pérez M, Prathep A, Robinson C, Romero J, Schmidt AL, Short FT, Van Tussenbroek BI, Santos R (2013) Effects of nutrient enrichment on seagrass population dynamics: evidence and synthesis from the biomass-density relationships. J Ecol 101:1552–1562. https://doi.org/10.1111/1365-2745.12134

Chavez PS Jr (1988) An improved dark-object subtraction technique for atmospheric scattering correction of multispectral data. Remote Sens Environ 24(3):459–479. https://doi.org/10.1016/0034-4257(88)90019-3

Congalton R, Green K (2008) Assessing the accuracy of remotely sensed data, principles and practices, 2nd edn. CRC Press, Boca Raton, p 200

Duarte CM, Marbà N, Gacia E, Fourqurean JW, Beggins J, Barrón C, Apostolaki ET (2010) Seagrass community metabolism: assessing the carbon sink capacity of seagrass meadows. Glob Biogeochem CyCles 24(4):GB4032. https://doi.org/10.1029/2010GB003793

Hedley JD, Harborne AR, Mumby PJ (2005) Simple and robust removal of sun glint for mapping shallow-water benthos. Int J Remote Sens 26(10):2107–2112. https://doi.org/10.1080/01431160500034086

Hochberg EJ, Atkinson MJ (2003) Spectral reflectance of coral reef bottom-types worldwide and implications for coral reef remote sensing. Remote Sens Environ 85(2):159–173. https://doi.org/10.1016/S0034-4257(02)00201-8

Kennedy H, Beggins J, Duarte CM, Fourqurean JW, Holmer M, Marbà N, Middelburg JJ (2010) Seagrass sediments as a global carbon sink: Isotopic constraints. Glob Biogeochem Cycles 24(4):GB4026. https://doi.org/10.1029/2010GB003848

Krause-Jensen D, Duarte C (2016) Substantial role of macroalgae in marine carbon sequestration. Nat Geosci 9:737–742. https://doi.org/10.1038/ngeo2790

Lavery PS, Mateo MÁ, Serrano O, Rozaimi M (2013) Variability in the carbon storage of seagrass habitats and its implications for global estimates of blue carbon ecosystem service. PLoS ONE 8(9):e73748. https://doi.org/10.1371/journal.pone.0073748

Lyimo LD (2016) Carbon sequestration processes in tropical seagrass beds. Ph.D. Thesis, Stockholm University, p 49

Lyzenga D (1981) Remote sensing of bottom reflectance and water attenuation parameters in shallow water using aircraft and Landsat data. Int J Remote Sens 2(1):71–82. https://doi.org/10.1080/01431168108948342

Mallombassi A, Mashoreng S, La Nafie YA (2020) The relationship between seagrass Thalassia hemprichii percentage cover and their biomass. Spermonde 6(1):7–10. https://doi.org/10.20956/jiks.v6i1.9922

McKenzie LJ, Finkbeiner MA, Kirkman H (2001) Methods for mapping seagrass distribution. In: Short FT, Coles RG (eds) Global seagrass research methods. Elsevier Science, pp 101–121. https://doi.org/10.1016/B978-044450891-1/50006-2

Pu R, Bell S, English D (2015) Developing hyperspectral vegetation indices for identifying seagrass species and cover classes. J Coast Res 31(3):595–615. https://doi.org/10.2112/JCOASTRES-D-12-00272.1

Roca G, Alcoverro T, Krause-Jensen D, Balsby TJS, van Katwijk MM, Marba N, Santos R, Arthur R, Mascaró O, Fernández-Torquemada Y, Pérez M (2016) Response of seagrass indicators to shifts in environmental stressors: a global review and management synthesis. Ecol Indic 63:310–323. https://doi.org/10.1016/j.ecolind.2015.12.007

Rohr ME, Bostrom C, Canal-Vergés P, Holmer M (2018) Blue carbon storage capacity of temperate Eeelgrass (*Zostera marina*) meadows. Glob Biogeochem Cy 32:1457–1475. https://doi.org/10.1029/2018GB005941

Waycott M, McMahon K, Mellors J, Calladine A, Kleine D (2004) A guide to tropical seagrass of the Indo-West Pacific. James Cook University, Townsville

Waycott M, Duarte CM, Carruthers TJB, Orth RJ, Dennison WC, Olyarnik S, Calladine A, Fourqurean JW, Heck KL, Hughes AR, Kendrick GA, Kenworthy WJ, Short FT, William SL (2009) Accelerating loss of seagrasses across the globe threatens coastal ecosystems. Proc Natl Acad Sci USA 106(30):12377–12381. https://doi.org/10.1073/pnas.0905620106

Zoffoli ML, Gernez P, Rosa P, Le Bris A, Brando VE, Barillé AL, Harin N, Peters S, Poser K, Spaias L, Peralta G (2020) Sentinel-2 remote sensing of Zostera noltei-dominated intertidal seagrass meadows. Remote Sens Environ 251:112020. https://doi.org/10.1016/j.rse.2020.112020